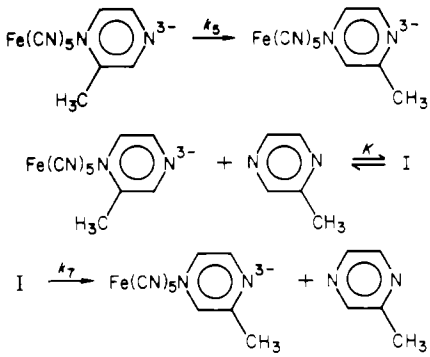

(5)

(6)

(7)

by eq 8. The first path in the proposed mechanism (eq 5)

$$k_{obsd} = \frac{k_5 + k_7K[\text{2-Mepyr}]}{1 + K[\text{2-Mepyr}]} \quad (8)$$

is a unimolecular linkage isomerization step, while the second is a bimolecular process involving rapid formation of an associative intermediate (eq 6) and its subsequent decomposition (eq 7). Values of k_5, k_7, and K computed by nonlinear least-squares analysis are respectively 0.8 ± 0.5 s^{-1}, 22 ± 10 s^{-1}, and 0.7 ± 0.4 M^{-1}. The rather wide error limits are highly correlated and due principally to the uncertainty in K. In particular, the presence of the k_5 term cannot be regarded as proved, and the value quoted is considered to be an upper limit. The line drawn in Figure 3, which fits the data well, was computed employing these rate and equilibrium constants.

Although the value of k_5 is an approximate one, it compares favorably with rate constants known for dissociation of several strained complexes of pentacyanoferrate(II). For example, k_d for the quinoxaline and the 2-cyanopyridine complexes are 0.62 and 1.1 s^{-1}, respectively.[14,15] For the hindered N-1 complex of histidine the specific rate is 0.109 s^{-1}.[16] Thus, our estimate of k_5 is in reasonable agreement with results for similar reactions.

Appearance of the [2-Mepyr]-dependent term in eq 8 is noteworthy because linkage isomerization reactions normally do not occur by bimolecular pathways for octahedral complexes.[17] However, in Table II evidence is presented that indicates a weak association between the free 2-Mepyr ligand and the parent pentacyano(2-methylpyrazine)iron(II) complex ion. In the table, one notes a growing shift in the MLCT band to longer wavelength as [2-Mepyr] is increased. The effect begins to be seen within the range of concentrations over which the second relaxation process was studied (0.1–0.9 M). We suggest that a weak charge-transfer interaction between bound and free 2-Mepyr molecules is responsible for the shifts in MLCT energies and that this interaction facilitates the linkage isomerization process.

Acknowledgment. This research was carried out, in part, at Brookhaven National Laboratory under contract with the U.S. Department of Energy and was supported by its Office of Basic Energy Sciences and was also supported, in part, by a University of Missouri Summer Faculty Fellowship (J.M.M.). Dr. Carol Creutz is thanked for her assistance in several laser flash experiments. Dr. Norman Sutin's kind hospitality at Brookhaven National Laboratory is gratefully acknowledged.

Registry No. I, 76299-52-0; $Fe(CN)_5(2\text{-Mepyr})^{3-}$, 60105-89-7; $Fe(CN)_5(OH_2)^{3-}$, 18497-51-3; 2-Mepyr, 109-88-0.

(14) Toma, H. E.; Coelho, A. L.; Malin, J. M., manuscript in preparation.
(15) Scecsy, A. P.; Miller, S. S.; Haim, A. *Inorg. Chim. Acta* **1978**, *28*, 189.
(16) Toma, H. E.; Martins, J. M.; Giesbrecht, E. *Inorg. Chim. Acta*, in press.
(17) Wilkins, R. G. "The Study of Kinetics and Mechanisms of Transition Metal Complexes"; Allyn and Bacon: Boston, 1974; Chapter 7.

Contribution from the Department of Chemistry, Purdue University, West Lafayette, Indiana 47907

Kinetics of the Oxidation of Iodide by the Nickel(III) Complex of Tri-α-aminoisobutyric Acid

JOHN M. T. RAYCHEBA and DALE W. MARGERUM*

Received June 30, 1980

The nickel(III)–deprotonated-peptide complex of tri-α-aminoisobutyric acid, Aib_3, oxidizes iodide by two reaction pathways to produce Ni(II) and I_3^-. The rate of loss of Ni(III) equals $2(k_C + k_C^H[H^+] + k_B/[Ni^{II}(H_{-2}Aib_3)^-])[I^-]^2[Ni^{III}(H_{-2}Aib_3)]^2$, where k_C, k_C^H, and k_B are 3.0×10^{10} M^{-3} s^{-1}, 3.8×10^{11} M^{-4} s^{-1}, and 2.5×10^5 M^{-2} s^{-1}, respectively. Path B, which is inhibited by excess Ni(II), occurs by two discrete one-electron-transfer steps and accounts for 30% or less of the observed rate. In the major reaction path (path C) two electrons are transferred in one concerted reaction step that proceeds by a transition-state complex composed of two nickel ions and two iodides.

Introduction

The nickel(III) complex of tri-α-aminoisobutyric acid Aib_3, I, has a Ni(III) → Ni(II) reduction potential, $E_{III,II}$, of 0.84

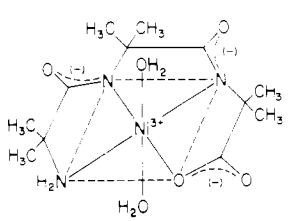

I $Ni^{III}(H_{-2}Aib_3)$

V (vs. NHE). In the absence of light this complex is kinetically resistant to acid, solvent substitution, and self-redox (intramolecular ligand oxidation) and is stable in neutral and acid solutions for extended periods of time (days to weeks).[1]

ESR,[2,3] electrochemical,[4–6] and crystallographic[7–9] studies of a wide variety of copper– and nickel–deprotonated-peptide

(1) Kirksey, S. T., Jr.; Neubecker, T. A.; Margerum, D. W. *J. Am. Chem. Soc.* **1979**, *101*, 1631.
(2) Lappin, A. G.; Murray, C. K.; Margerum, D. W. *Inorg. Chem.* **1978**, *17*, 1630.
(3) Falk, K. E.; Freeman, H. C.; Jansson, T.; Malmström, B. G.; Vänngard, T. *J. Am. Chem. Soc.* **1967**, *89*, 6071.
(4) Youngblood, M. P.; Margerum, D. W. *Inorg. Chem.* **1980**, *19*, 3068.
(5) Bossu, F. P.; Margerum, D. W. *Inorg. Chem.* **1977**, *16*, 1210.
(6) Bossu, F. P.; Chellappa, K. L.; Margerum, D. W. *J. Am. Chem. Soc.* **1977**, *99*, 2195.
(7) Freeman, H. C.; Schoone, J. C.; Sime, J. G. *Acta Crystallogr.* **1965**, *18*, 381.
(8) Freeman, H. C.; Guss, J. M.; Sinclair, R. L. *Chem. Commun.* **1968**, 485.
(9) Lim, M. C.; Sinn, E.; Martin, R. B. *Inorg. Chem.* **1976**, *15*, 807.

0020-1669/81/1320-1441$01.25/0

complexes similar to I have shown that the d^7 nickel(III) and d^9 copper(II) complexes have square-pyramidal or tetragonally distorted octahedral geometries, while the d^8 nickel(II) and copper(III) complexes have square-planar geometries. Thus, in aqueous solution the one-electron reduction of a nickel(III)–peptide complex, such as I, is accompanied by a tetragonal to square planar (tetr → sp) conversion and the liberation of two water molecules that were axially coordinated to the nickel(III) (eq 1). The reduction of a copper(III)–

$$Ni^{III}(H_{-2}Aib_3)(H_2O)_2 + e^- \rightleftarrows Ni^{II}(H_{-2}Aib_3)^- + 2H_2O \quad (1)$$

peptide complex, $Cu^{III}(H_{-n}L)$, results in an opposite (sp → tetr) geometry change (eq 2). The solvent and temperature de-

$$Cu^{III}(H_{-n}L) + 2H_2O + e^- \rightleftarrows Cu^{II}(H_{-n}L)(H_2O)_2^- \quad (2)$$

pendences of $E_{III,II}$ for eq 1 and 2 have clearly demonstrated the importance of the geometry and coordination changes to the thermodynamics of reactions that involve the copper(III,II) and nickel(III,II) redox couples.[3] The solvent accessibility of the axial coordination sites has also been shown to affect the acid dissociation and nucleophilic ligand-exchange reactions of the deprotonated nickel(II)–peptide complexes.[10] Thus, the geometry and coordination changes that accompany the redox reactions of the copper- and nickel–deprotonated-peptide complexes should also affect the kinetics of these redox reactions.

The oxidation of iodide to iodine and triiodide by $Ni^{III}(H_{-2}Aib_3)$ is a thermodynamically favorable reaction (eq 3)

$$2Ni^{III}(H_{-2}Aib_3) + 2I^- \rightleftarrows 2Ni^{II}(H_{-2}Aib_3)^- + I_2$$
$$I_2 + I^- \rightleftarrows I_3^- \quad (3)$$

that exhibits the same 2:1 [M(III) reduced]:[($I_2 + I_3^-$) produced] stoichiometry as is observed for the analogous copper(III) reactions. The copper(III)–deprotonated-peptide complexes, $Cu^{III}(H_{-n}L)$, oxidize iodide to iodine by two reaction pathways, A and B. The rates of both pathways are first order with respect to the Cu(III) oxidant. Path A is also first order in $[I^-]$, while path B exhibits a second-order iodide dependence.[11] The kinetics of reaction 3 differ from those of the analogous copper(III) reactions in that the observed reactions are second order with respect to the Ni(III) oxidant, $Ni^{III}(H_{-2}Aib_3)$, concentration. Also, under comparable conditions ($[M(III)] = 2 \times 10^{-5}$ M and $[I^-] = 10^{-3}$–0.1 M), the rates as measured by the first half-life are 30–100 times faster for the Ni(III) reactions. On the other hand, the kinetics of reaction 3 are similar to the analogous copper(III) reactions in that two reaction pathways, B and C, are observed. Although the oxidant reaction-rate orders are different for the nickel(III) reaction (eq 3), reaction path B is proposed to proceed via the formation of an I_2^- radical anion intermediate. This reaction path is common to both the copper(III) and nickel(III) oxidations of iodide.

Experimental Section

Tri-α-aminoisobutyric acid monohydrate, $Aib_3 \cdot H_2O$, was synthesized as previously described.[12] Stock $Ni(ClO_4)_2$ solutions were prepared from the twice-recrystallized salt, and the $NaClO_4$ solutions were prepared from analytical reagent grade Na_2CO_3 and perchloric acid. Solutions of the deprotonated nickel(II)–Aib_3 complex, $[Ni^{II}(H_{-2}Aib_3)]^-$, were prepared by the slow addition of 0.1 N NaOH to a solution that contained a 1:1.1 to 1:1.2 mole ratio of $Ni(ClO_4)_2$ and Aib_3. Prior to the electrochemical oxidation the pH was adjusted to 6.5–7. The $Ni^{III}(H_{-2}Aib_3)$ solutions were prepared by electrochemical oxidation of the nickel(II) solutions at 0.9 V vs. Ag/AgCl (3 M NaCl) reference with use of a flow-through system that included a graphite-powder working electrode.[13] The efficiency of this oxidation varied from 60 to 90%. The $Ni^{III}(H_{-2}Aib_3)$ solutions were deoxygenated by vigorous bubbling with Ar(g) and were protected from light. The NaI solutions were prepared immediately prior to each kinetic experiment and were similarly deoxygenated. Hydrogen ion concentrations were obtained from the measured pH after calibrating the pH meter with standard acid solutions of ionic strength 1.0 ($NaClO_4$).

Table I. Dependence of the Observed Second-Order Rate Constant on the Iodide Concentration for the Oxidation of Iodide by $Ni^{III}(H_{-2}Aib_3)$[a]

$-\log [H^+]$	$10^3[I^-]$, M	k_{obsd}, M^{-1} s^{-1}
5.21[b]	1.00	$(4.79 \pm 0.05) \times 10^4$
5.22[b]	2.00	$(1.74 \pm 0.03) \times 10^5$
5.20[c]	3.00	$(3.43 \pm 0.04) \times 10^5$
5.20[b]	4.00	$(6.85 \pm 0.35) \times 10^5$
5.19[c]	6.00	$(1.40 \pm 0.02) \times 10^6$
5.20[c]	8.00	$(2.40 \pm 0.05) \times 10^6$
5.18[b]	10.0	$(3.9 \pm 0.2) \times 10^6$
5.19[b]	14.0	$(7.6 \pm 0.3) \times 10^6$
5.18[c]	16.0	$(9.6 \pm 0.4) \times 10^6$
5.21[b]	20.0	$(1.6 \pm 0.1) \times 10^7$
1.01	1.00	$(8.8 \pm 0.1) \times 10^4$
1.01	2.00	$(4.1 \pm 0.3) \times 10^5$
1.01	3.00	$(7.2 \pm 0.2) \times 10^5$
1.01	4.00	$(1.59 \pm 0.05) \times 10^6$
1.01	8.00	$(7.0 \pm 0.4) \times 10^6$

[a] $\mu = 1.0$ ($NaClO_4$), 25.0 °C, $[acetate]_T = 0.01$ M, $\lambda = 353$ nm. [b] $[Ni^{III}(H_{-2}Aib_3)]_{init} = 2.0 \times 10^{-5}$ M, $[Ni^{II}(H_{-2}Aib_3)^-]_{av} = 2.0 \times 10^{-5}$ M. [c] $[Ni^{III}(H_{-2}Aib_3)]_{init} = 4.7 \times 10^{-5}$ M, $[Ni^{II}(H_{-2}Aib_3)^-]_{av} = 3.6 \times 10^{-5}$ M.

The kinetics of the $Ni^{III}(H_{-2}Aib_3)$ oxidation of iodide were spectrophotometrically monitored at 353 nm with use of a Durrum stopped-flow spectrophotometer. (For I_3^- $\lambda_{max} = 353$ nm and $\epsilon = 2.64 \times 10^4$ M^{-1} cm^{-1},[14] and for $Ni^{III}(H_{-2}Aib_3)$ $\lambda_{max} = 352$ nm and $\epsilon = 3.6 \times 10^3$ M^{-1} cm^{-1}.[12]) All reactions were run under irreversible pseudo-second-order conditions at 25.0 °C and an ionic strength of 1.0 ($NaClO_4$). The absorbance–time data were collected with an on-line digital computer[15] and were subsequently analyzed in an off-line mode. All reactions were pseudo second order in the limiting reagent, $Ni^{III}(H_{-2}Aib_3)$, and conformed to the rate expression in eq 4.

$$-\frac{d}{dt}[Ni^{III}(H_{-2}Aib_3)] = 2k_{obsd}[Ni^{III}(H_{-2}Aib_3)]^2 \quad (4)$$

The observed second-order rate constant, k_{obsd}, was obtained from a linear-least-squares analysis of eq 5, where $\Delta\epsilon$ is the molar ab-

$$\frac{1}{A_\infty - A} = \frac{-2k_{obsd}}{(\Delta\epsilon)l}t + \frac{1}{A_\infty - A_0} \quad (5)$$

sorptivity difference per equivalent ($\epsilon_p/2 - \epsilon_{Ni(III)}$), l is the cell path length (cm), and A, A_0, and A_∞ are the absorbances at time t, zero, and infinity, respectively. The molar absorptivity of the iodine–triiodide product, ϵ_p, depends on the iodide concentration and is given by eq 6, where K is $[I_3^-]/[I_2][I^-]$. The reported values of k_{obsd} are the mean of at least four replicates.

$$\epsilon_p = \frac{\epsilon_{I_3^-}K[I^-]}{1 + K[I^-]} \quad (6)$$

Results

The stoichiometry of the overall reaction was spectrophotometrically confirmed to be as indicated by eq 3. The rate of the oxidation of iodide by $Ni^{III}(H_{-2}Aib_3)$ was second order with respect to the limiting reagent, $Ni^{III}(H_{-2}Aib_3)$, and the observed second-order rate constant, k_{obsd}, is independent of

(10) Raycheba, J. M. T.; Margerum, D. W. *Inorg. Chem.* **1980**, *19*, 837.
(11) Raycheba, J. M. T.; Margerum, D. W. *Inorg. Chem.* **1981**, *20*, 45.
(12) Kirksey, S. T., Jr.; Neubecker, T. A.; Margerum, D. W. *J. Am. Chem. Soc.* **1979**, *101*, 1631.
(13) Clark, B. R.; Evans, D. H. *J. Electroanal. Chem. Interfacial Electrochem.* **1976**, *69*, 181.
(14) Awtrey, A. D.; Connick, R. E. *J. Am. Chem. Soc.* **1951**, *73*, 1842.
(15) Willis, B. G.; Bittikoffer, J. A.; Pardue, H. L.; Margerum, D. W. *Anal. Chem.* **1970**, *42*, 1430.

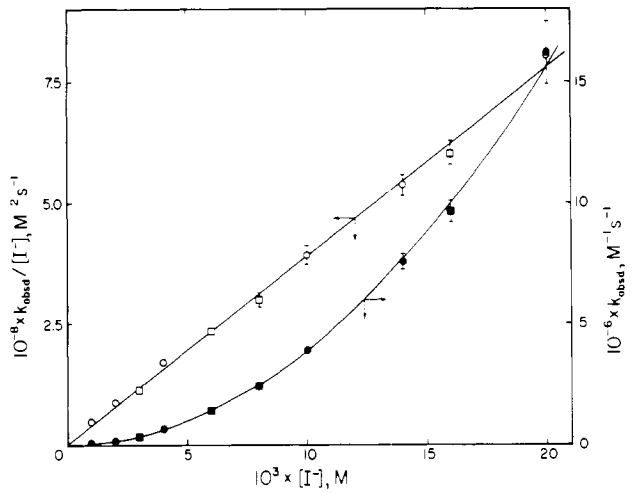

Figure 1. Iodide dependence of the observed second-order rate constant for the reaction of $Ni^{III}(H_{-2}Aib_3)$ with I^-.

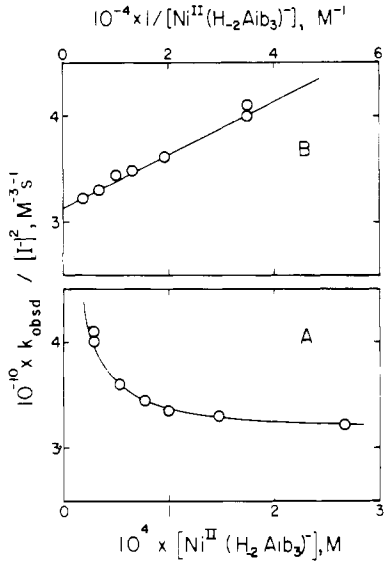

Figure 2. Dependence of the observed second-order rate constant on the concentration of added $Ni^{II}(H_{-2}Aib_3)^-$.

Table II. Dependence of the Observed Second-Order Rate Constant on the Concentration of Added $Ni^{II}(H_{-2}Aib_3)^-$ [a]

$-\log [H^+]$	$10^5 \times [Ni^{II}(H_{-2}Aib_3)^-]_{av}$, M	$10^{-4}k_{obsd}$, M^{-1} s^{-1}
6.12	2.8	4.1 ± 0.1
6.10	2.8	4.00 ± 0.02
6.14	5.2	3.61 ± 0.05
6.12	7.6	3.42 ± 0.05
6.18	10.0	3.35 ± 0.10
6.20	14.7	3.30 ± 0.05
6.51	26.6	3.22 ± 0.04

[a] $[Ni^{III}(H_{-2}Aib_3)]_0 = 9.2 \times 10^{-5}$ M, $[I^-] = 1.00 \times 10^{-3}$ M, μ = 1.0 ($NaClO_4$), $[acetate]_T = 0.01$ M, 25.0 °C, λ = 353 nm.

the initial $Ni^{III}(H_{-2}Aib_3)$ concentration. However, k_{obsd} does depend on the iodide, excess $Ni^{II}(H_{-2}Aib_3)^-$, and hydrogen ion concentration. Under all reaction conditions, the reaction rate increases as the square of the iodide concentration (Table I and Figure 1) and is suppressed by excess $Ni^{II}(H_{-2}Aib_3)^-$ (Table II). At high $Ni^{II}(H_{-2}Aib_3)^-$ concentrations k_{obsd} approaches a limiting value (Figure 2).

The lack of complete suppression indicates that the $Ni^{III}(H_{-2}Aib_3)$–I^- reaction proceeds by two reaction pathways, B and C, which exhibit different nickel(II) dependences. Path C is unaffected by the $Ni^{II}(H_{-2}Aib_3)^-$ concentration, while path B exhibits an inverse first-order $[Ni^{II}(H_{-2}Aib_3)^-]$ dependence (Figure 2). In the presence of excess $Ni^{II}(H_{-2}Aib_3)^-$ the reaction rate is determined solely by path C. The pH dependence of path C was determined in the presence of a large excess of $Ni^{II}(H_{-2}Aib_3)^-$ (Table III). Path C exhibits both a pH-independent term and a first-order $[H^+]$ dependence (Figure 3).

Table III. pH Dependence of the Observed Second-Order Rate Constant for the Oxidation of Iodide by $Ni^{III}(H_{-2}Aib_3)$ [a]

$-\log [H^+]$	10^4k_{obsd}, M^{-1} s^{-1}	$-\log [H^+]$	10^4k_{obsd}, M^{-1} s^{-1}
0.77	9.4 ± 0.1	2.37 [b]	3.1 ± 0.1
0.98	7.0 ± 0.2	2.46	3.3 ± 0.1
1.16	6.1 ± 0.2	3.09 [b]	3.12 ± 0.03
1.16	5.15 ± 0.05	4.07 [b]	2.95 ± 0.08
1.49	4.10 ± 0.07	4.42 [c]	2.75 ± 0.07
1.83	3.65 ± 0.05	5.02 [c]	2.8 ± 0.1
2.13	3.40 ± 0.05		

[a] $[Ni^{III}(H_{-2}Aib_3)]_0 = 2.5 \times 10^{-5}$ M, $[Ni^{II}(H_{-2}Aib_3)^-]_0 = 3.2 \times 10^{-4}$ M. $[I^-] = 1.00 \times 10^{-3}$ M, μ = 1.0 ($NaClO_4$), 25.0 °C, λ = 390 nm. [b] $[ClCH_2CO_2^-]_T = 0.005$ M. [c] $[acetate]_T$ = 0.01 M.

Table IV. Measured and Calculated Constants for the Oxidation of Iodide by $Ni^{III}(H_{-2}Aib_3)$ [a]

constant	value
$K_0^2k_1$ (k_C), M^{-3} s^{-1}	$(3.0 \pm 0.1) \times 10^{10}$
k_{-1}, M^{-2} s^{-1}	10^3
$K_0K_0'K_{1H}k_2$ (k_C^H), M^{-4} s^{-1}	$(3.8 \pm 0.1) \times 10^{11}$
K_{1H}, M^{-1}	≤ 5
$K_0K_3k_4$ (k_B), M^{-2} s^{-1}	$(2.5 \pm 0.1) \times 10^5$
k_{-4}, M^{-1} s^{-1}	9×10^{-3}
k_4, M^{-1} s^{-1}	6×10^6
K_0K_3, M^{-1}	4×10^{-2}
K_0, M^{-1}	≤ 10
K_4	6.8×10^8
$K_0K_3K_4$ and $K_0^2K_1$, M^{-1}	2.8×10^7
$E^\circ(Ni^{III,II}(H_{-2}Aib_3)^{0,-})$, V	0.84 [b]
$E^\circ(I_2/2I^-)$, V	0.6197 [c]
$E^\circ(I_2^-/2I^-)$, V	≤ 0.92 [d]

[a] μ = 1.0 ($NaClO_4$), 25 °C. [b] Reference 1. [c] Latimer, W. M. "Oxidation Potentials", 2nd ed.; Prentice-Hall: Englewood Cliffs, NJ, 1952; p 64. [d] Reference 11.

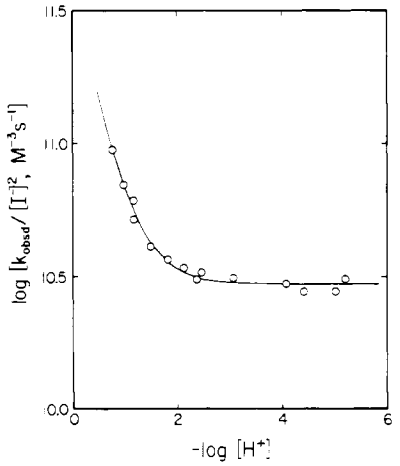

Figure 3. pH dependence of reaction path C for the oxidation of iodide by $Ni^{III}(H_{-2}Aib_3)$.

The iodide, $[Ni^{II}(H_{-2}Aib_3)^-]$, and $[H^+]$ dependences lead to the expression given in eq 7 for the observed second-order

$$k_{obsd} = (k_C + k_C^H[H^+] + k_B/[Ni^{II}(H_{-2}Aib_3)^-])[I^-]^2 \quad (7)$$

rate constant, k_{obsd}. A least-squares analysis was used to obtain

the resolved values of the rate constants k_C, k_C^H, and k_B. The results of that analysis are $k_C = (3.0 \pm 0.1) \times 10^{10}$ M^{-3} s^{-1}, $k_C^H = (3.8 \pm 0.1) \times 10^{11}$ M^{-4} s^{-1}, and $k_B = (2.5 \pm 0.1) \times 10^5$ M^{-2} s^{-1}.

Discussion

$Ni^{III}(H_{-2}Aib_3)$ Reactions. The mechanism proposed for the $Ni^{III}(H_{-2}Aib_3)$ oxidation of iodide is given in eq 8–15. The

$$Ni^{III}(H_{-2}Aib_3) + I^- \overset{K_0}{\rightleftharpoons} [Ni^{III}(H_{-2}Aib_3)(I^-)] \quad (8)$$

$$2[Ni^{III}(H_{-2}Aib_3)(I^-)] \underset{k_{-1}}{\overset{k_1}{\rightleftharpoons}} 2Ni^{II}(H_{-2}Aib_3)^- + I_2 \quad (9)$$

$$Ni^{III}(H_{-2}Aib_3) + H^+ \overset{K_{1H}}{\rightleftharpoons} Ni^{III}(H_{-2}Aib_3)\cdot H^+ \quad (10)$$

$$Ni^{III}(H_{-2}Aib_3)\cdot H^+ + I^- \overset{K_0'}{\rightleftharpoons} [Ni^{III}(H_{-2}Aib_3)(H^+)(I^-)] \quad (11)$$

$$[Ni^{III}(H_{-2}Aib_3)(H^+)(I^-)] + Ni^{III}(H_{-2}Aib_3)(I^-) \underset{k_{-2}}{\overset{k_2}{\rightleftharpoons}} Ni^{II}(H_{-2}Aib_3)\cdot H + Ni^{II}(H_{-2}Aib_3)^- + I_2 \quad (12)$$

$$Ni^{III}(H_{-2}Aib_3)(I^-) + I^- \underset{k_{-3}}{\overset{k_3}{\rightleftharpoons}} Ni^{II}(H_{-2}Aib_3)^- + I_2^- \quad (13)$$

$$I_2^- + Ni^{III}(H_{-2}Aib_3) \underset{k_{-4}}{\overset{k_4}{\rightleftharpoons}} Ni^{II}(H_{-2}Aib_3)^- + I_2 \quad (14)$$

$$I_2 + I^- \rightleftarrows I_3^- \quad (15)$$

rate-determining reaction steps occur in eq 9, 12, and 14 and were effectively irreversible under the experimental conditions used. In terms of this mechanism, the observed second-order rate constant, k_{obsd}, is given by eq 16. The experimental data

$$k_{obsd} = \{[K_0^2k_1/(1 + K_0[I^-]) + K_0K_0'K_{1H}k_2[H^+]/(1 + K_0'[I^-])][I^-]^2\}/\{(1 + K_0[I^-])(1 + K_{1H}[H^+])\} + K_0k_3k_4[I^-]^2/\{(1 + K_0[I^-])^2(k_{-3}[Ni^{II}(H_{-2}Aib_3)^-] + k_4[Ni^{III}(H_{-2}Aib_3)])\} \quad (16)$$

indicate that three approximations can be made to simplify eq 16. (1) The $[I^-]^2$ dependence is maintained throughout the entire iodide concentration range (Figure 1), indicating that $K_0[I^-] \ll 1$ and that $K_0 \leq 10$ M^{-1}. That is, the $[Ni^{III}(H_{-2}Aib_3)(I^-)]$ species formed in eq 8 is present as a steady-state species and is not formed in appreciable concentrations. The observations that 1 M Cl^- has little if any effect on the UV–vis absorption spectrum of $Ni^{III}(H_{-2}Aib_3)$ and no effect on the electrochemical behavior (cyclic voltammetry) of $Ni^{III,II}(H_{-2}Aib_3)$ provide additional support for the assumption that K_0 is less than 10 M^{-1}. Also, added sulfate ion (up to 0.1 M) has no effect on the rate of oxidation of iodide by $Ni^{III}(H_{-2}Aib_3)$. (2) At the highest acid concentrations used, no deviation from the first-order H^+ dependence is detectable (Figure 3), and, therefore, $K_{1H}[H^+] \ll 1$ and $K_{1H} \leq 5$ M^{-1}. This is also supported by the observation that the UV–vis spectra of $Ni^{III}(H_{-2}Aib_3)$ at pH 5 (μ = 1.0 M $NaClO_4$) and in 1 M $HClO_4$ are almost identical. (3) A plot (Figure 2) of k_{obsd} vs. $1/[Ni^{II}(H_{-2}Aib_3)^-]$ of the data in Table II is linear, indicating that, under the reaction conditions used, $k_{-3}[Ni^{II}(H_{-2}Aib_3)^-] \gg k_4[Ni^{III}(H_{-2}Aib_3)]$. This approximation will break down at very low $[Ni^{II}(H_{-2}Aib_3)]$, and deviations from pseudo-second-order kinetic behavior can be expected. However, due to unavoidable inefficiencies in the preparation of the $Ni^{III}(H_{-2}Aib_3)$ reagent, some $Ni^{II}(H_{-2}Aib_3)^-$ was always present in the reactant solutions. No measurable deviations from pseudo-second-order kinetics were detected under any of the experimental conditions used.

Substitution of the approximations (1)–(3) into eq 16 leads to the simplified expression for k_{obsd} given in eq 17, where K_3 is k_3/k_{-3}. The rate constants k_C and k_C^H, which describe reaction path C (eq 8–12), are $K_0^2k_1$ and $K_0K_0'K_{1H}k_2$, respectively. The rate constant k_B, which accounts for the kinetics of reaction path B (eq 8, 13, and 14), is $K_0K_3k_4$. The resolved values for these rate constants as well as the calculated values for a number of other rate and equilibrium constants are listed in Table IV.

$$k_{obsd} = \left(K_0^2k_1 + K_0K_0'K_{1H}k_2[H^+] + \frac{K_0K_3k_4}{[Ni^{II}(H_{-2}Aib_3)^-]}\right)[I^-]^2 \quad (17)$$

The major kinetic pathway (path C) for the oxidation of iodide by $Ni^{III}(H_{-2}Aib_3)$ accounts for 70% or more of the observed rate (Figure 2) and consists of a pH-independent (eq 8 and 9) as well as a pH-dependent part. Both exhibit second-order [Ni(III)] and second-order $[I^-]$ reaction-rate dependences, indicating that reaction path C proceeds via a transition-state complex that is composed of two nickel ions and two iodide ions or atoms. Such a transition-state complex (II) can facilitate the two-electron transfer that is required

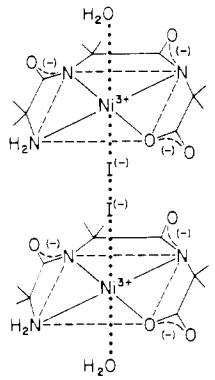

II Suggested Transition-State Complex for Reaction Path C.

in order to form the iodine product. Nickel(II) and I· or I_2^- radical intermediates are not generated in the course of reaction path C and this reaction path does not involve discrete one-electron-transfer steps. Instead, the two-electron oxidation is accomplished in one concerted reaction step (eq 9).

Outside-protonated species that are formed by the rapid protonation of a peptide oxygen without the cleavage of the metal–N(peptide) bond have been observed as intermediates in the acid decomposition reactions of a wide variety of Ni(II)–, Cu(II)–, Cu(III)–, and Pd(II)–peptide complexes.[10,11,16–18] The formation of such an outside-protonated species, $[Ni^{III}(H_{-2}Aib_3)\cdot H]^+$, is proposed in eq 10 to account for the increased reaction rate in acid. Since only a first-order $[H^+]$ dependence is observed, the nickel(III) reactant is not fully converted to its protonated form even at $-\log [H^+] = 0.77$. Hence the protonation constant, K_{1H} (eq 10), is less than 5 M^{-1}. The value of K_{1H} for most of the peptide and peptide amide complexes of copper(II), nickel(II), and cobalt(III) is normally in the range of $10^{1.5}$–10^3 M^{-1}. However, the outside-protonation constant for the ternary complex that is formed from Ni(II), diglycinamide, and 2,6-dimethylpyridine (lut), $Ni^{II}(H_{-2}G_2a)$lut, is also less than 5 M^{-1}.[10]

The rate of the minor kinetic pathway (path B) for the oxidation of iodide by $Ni^{III}(H_{-2}Aib_3)$ is suppressed by the

(16) Rybka, J. S.; Kurtz, J. L.; Neubecker, T. A.; Margerum, D. W. *Inorg. Chem.* **1980**, *19*, 2791.
(17) Raycheba, J. M. T.; Margerum, D. W. *Inorg. Chem.* **1980**, *19*, 497.
(18) Cooper, J. C.; Wong, L. F.; Margerum, D. W. *Inorg. Chem.* **1978**, *17*, 261.

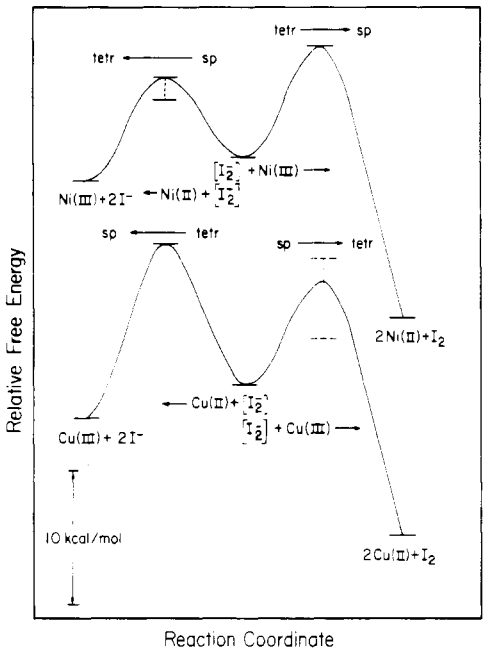

Figure 4. Reaction path B reaction-coordinate diagrams for the oxidation of iodide by $Ni^{III}(H_{-2}Aib_3)$ and $Cu^{III}(H_{-2}A_3)$, where A_3 is tri-L-alanine.

$Ni^{II}(H_{-2}Aib_3)^-$ product (eq 13) and accounts for less than 30% of the overall rate (Table II, Figure 2). In contrast to the major path, reaction path B does proceed via discrete one-electron-transfer steps (eq 13 and 14). The oxidation of iodide by such diverse oxidants as Cu(III)–peptide complexes,[11] Ni(III)–macrocycle complexes,[19-21] $Fe(phen)_3^{3+}$,[22,23] $IrCl_6^{2-}$,[22] and $Fe(aq)^{3+}$ [24] also exhibit $[I^-]^2$ rate dependences and have been proposed to occur by reaction sequences directly analogous to eq 8, 13, and 14. For all but three of the Ni(III)–macrocycle oxidants[19,20] the oxidation of the I_2^- radical intermediate (eq 14) is more rapid than its reduction (eq 13). Consequently, the rate expression typically obtained for path B is rate = $k[Ox][I^-]^2$. The $[Ni(III)]^2$ and $[Ni(II)]^{-1}$ dependences that are observed in the present case indicate that the rate-determining step for the $Ni^{III}(H_{-2}Aib_3)$ reaction is occurring at a later stage in the reaction sequence than it does with most other oxidants. That is, the rate-determining step occurs during the reduction of the second nickel(III) rather than the first.

In our earlier study[11] of the oxidation of iodide by the copper(III)–deprotonated-peptide complexes, $Cu^{III}(H_{-n}L)$, the rate of reaction via path B was not limited by the rate of electron transfer. Instead, it was suggested that the change in axial coordination that accompanied the conversion of the square-planar (sp) d^8 Cu(III) complex to a tetragonally distorted (tetr) d^9 Cu(II) complex made an important contribution to the magnitude of the activation barrier.[11] The tetr to sp geometry change that accompanies the reduction of $Ni^{III}(H_{-2}Aib_3)$ is the reverse of that observed for the reduction of the $Cu^{III}(H_{-n}L)$ complexes. The geometry changes that occur at each stage of reaction path B for the copper(III) and nickel(III) oxidations of iodide are indicated in the reaction-coordinate diagram given in Figure 4.

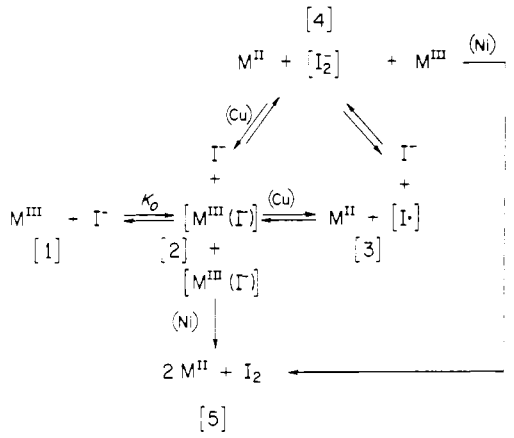

Figure 5. General reaction scheme for the oxidation of iodide by the Cu(III)- and Ni(III)–peptide complexes. The rate-determining steps are indicated by (Cu) for the copper(III) reactions and by (Ni) for the nickel(III) reactions. The three reaction path sequences are as follows: path A, [1] → [2] → [3] → [4] → [5]; path B, [1] → [2] → [4] → [5]; path C, [1] → [2] → [5].

The most important features of the reaction-coordinate diagram (Figure 4) can best be seen by considering the two possible reactions of the I_2^- radical anion intermediate. Both the reduction of I_2^- and its oxidation are thermodynamically favorable processes. When the reduction of I_2^- is more facile than its oxidation to I_2, the reaction rate exhibits a second-order oxidant dependence. This is the case for the $Ni^{III}(H_{-2}Aib_3)$ reaction. During the slow step ($I_2^- \rightarrow I_2$) the nickel(III)–Aib_3 complex undergoes a tetr to sp coordination change. On the other hand, the reduction of I_2^- to I^- rather than its oxidation to I_2 is the slow step for the copper reactions. A tetr to sp geometry change also occurs in the course of this reaction. Thus, when copper- and nickel–peptide complexes oxidize or reduce I_2^-, the slower reaction (larger activation barrier) is the one that is accompanied by a tetragonal to square-planar geometry change.

General Reaction Scheme. The kinetics of the oxidation of iodide by the copper(III)- and nickel(III)–peptide complexes show some similarities and some differences. The three reaction pathways, A, B, and C, that have been observed for these reactions can be combined into one general reaction scheme as shown in Figure 5. This scheme is appropriate not only for the oxidation of iodide by the Cu(III)- and Ni(III)–peptide complexes but also for the oxidation of I^- and other halides and pseudohalides (e.g., SCN^-) by oxidants such as $Fe(phen)_3^{3+}$,[22,23] $Os(phen)_3^{3+}$,[5] $IrCl_6^{2-}$,[22] $Co(aq)^{3+}$,[26] $Fe(aq)^{3+}$,[24] and Ni(III)–macrocycle complexes.[19,21,27] In Figure 5, the overall reaction proceeds from state [1] to state [5] and the rate-determining steps are indicated by a (Cu) for the copper(III)–peptide reactions and a (Ni) for the nickel(III)–peptide reactions. Reaction path A proceeds via states [1], [2], [3], [4], and [5], while path B occurs via [1], [2], [4], and [5] and path C proceeds by states [1], [2], and [5].

The kinetics of the Cu(III)- and Ni(III)–peptide oxidations of iodide differ in three respects. (1) The nickel reactions are second order in Ni(III), while the copper reactions are first order in Cu(III). (2) Although path B is common to both the Cu(III) and Ni(III) reactions, path A is not observed in the $Ni^{III}(H_{-2}Aib_3)$ reactions. (3) Path C is the major kinetic pathway for the nickel(III) reaction but does not carry a measurable amount of the rate in the copper(III) reactions. These apparent differences are accounted for by the general

(19) Whitburn, K. D.; Laurence, G. S. *J. Chem. Soc., Dalton Trans.* **1979**, *139*.
(20) Jaacobi, M.; Meyerstein, D.; Lilie, J. *Inorg. Chem.* **1979**, *18*, 429.
(21) Haines, R. I.; McAuley, A. *Inorg. Chem.* **1980**, *19*, 719.
(22) Adedinsewo, C. O.; Adegite, A. *Inorg. Chem.* **1979**, *18*, 3597.
(23) Ige, J.; Ojo, J. F.; Obubuyide, O. *Can. J. Chem.* **1979**, *57*, 2065.
(24) Laurence, G. S.; Ellis, K. J. *J. Chem. Soc., Dalton Trans.* **1972**, 2229.
(25) Nord, G.; Pedersen, B.; Farver, O. *Inorg. Chem.* **1979**, *18*, 3597.
(26) Davies, G.; Watkins, K. O. *J. Phys. Chem.* **1970**, *74*, 3388.
(27) Maruthamuthu, P.; Patterson, L. K.; Ferraudi, G. *Inorg. Chem.* **1978**, *17*, 3157.

reaction scheme proposed in Figure 5.

In path B, the rate-determining step for the $Ni^{III}(H_{-2}Aib_3)$ reaction occurs at a later stage in the reaction sequence ([4] → [5] in Figure 5) than it does for the copper(III)–peptide oxidations of iodide. Also, path C, which will always exhibit a second-order dependence on the oxidant, carries the majority of the $Ni^{III}(H_{-2}Aib_3)$–I^- reaction rate but is not present in the Cu(III) reactions. Thus, the oxidant reaction-rate order differences are attributable to the fact that the rate-determining step occurs at a later stage (between [4] and [5] in Figure 5) in the reaction sequence [1], [2], [4], and [5] when the oxidant is $Ni^{III}(H_{-2}Aib_3)$ rather than a copper(III)–peptide complex. The differing locations of the rate-determining steps also account for the apparent absence of reaction path A when $Ni^{III}(H_{-2}Aib_3)$ is the oxidant. Because the rate-determining step occurs late in the reaction sequence, the rate dependences of path A and path B are identical. That is, the two reaction paths, A and B, that are kinetically distinguishable in the copper(III)–peptide oxidations of iodide are merged into one combined reaction path, B, in the $Ni^{III}(H_{-2}Aib_3)$ reactions. Finally, the $M^{III}(I^-)$ species ([2] in Figure 5) is not formed in appreciable concentrations. Path C ([1] → [2] → [5]) involves the reaction of two $M^{III}(I^-)$ species, and as a consequence the rate of reaction via path C is very sensitive to the magnitude of the equilibrium constant K_0. The tetragonal d^7 nickel(III)–deprotonated peptide complexes of triglycinamide and *N,N'*-diglycylethylenediamine readily form axial adducts with ligands such as NH_3 and imidazole at room temperature and chloride in frozen (N_2(l)) aqueous glasses.[2,28] In contrast, the analogous adducts with the square-planar, d^8 copper(III) deprotonated peptides have not been detected. Thus, the equilibrium constant, K_0, is expected to be smaller for the copper(III) peptides than for the nickel(III) peptides. As a consequence, reaction paths A and B dominate the kinetics of the Cu(III) oxidations of iodide, while path C is the major kinetic pathway for the Ni(III) oxidation of iodide.

(28) Murray, C. K.; Margerum, D. W., to be submitted for publication.

Conclusions

The oxidation of iodide to iodine by the nickel(III) complex of tri-α-aminoisobutyric acid, $Ni^{III}(H_{-2}Aib_3)$, is a thermodynamically favorable reaction that occurs by two kinetic pathways. Both pathways exhibit second-order Ni(III) and iodide dependences. The major pathway, path C, proceeds via a transition-state complex composed of two nickel–Aib_3 complexes and two iodides. The two-electron exchange between the two Ni(III) complexes and the two iodides is accomplished in one concerted reaction step. The minor reaction pathway, path B, is inhibited by the $Ni^{II}(H_{-2}Aib_3)^-$ product and proceeds via two discrete one-electron-transfer steps. The first step produces an I_2^- radical anion and $Ni^{II}(H_{-2}Aib_3)^-$. In contrast to the copper(III) reactions, the reduction of I_2^- by Ni(II) is faster than the oxidation of I_2^- to I_2 by the second equivalent of $Ni^{III}(H_{-2}Aib_3)$, and a second-order Ni(III) rate dependence is observed.

Acknowledgment. This investigation was supported by Public Health Service Grant No. GM12152 from the National Institute of General Medical Sciences. The authors thank A. Hamburg for synthesizing the tri-α-aminoisobutyric acid.

Registry No. $Ni^{III}(H_{-2}Aib_3)(H_2O)_2$, 76757-47-6; I^-, 20461-54-5; $Ni^{II}(H_{-2}Aib_3)^-$, 76757-48-7; I_3^-, 14900-04-0.

Contribution from the Department of Chemistry, Purdue University, West Lafayette, Indiana 47907

Rapid Electron-Transfer Reactions between Hexachloroiridate(IV) and Copper(II) Peptides

GROVER D. OWENS and DALE W. MARGERUM*

Received July 30, 1980

The rates of oxidation of 12 copper(II)–peptide complexes by $IrCl_6^{2-}$ to give the copper(III) complexes are measured with use of a pulsed-flow spectrometer. The resulting second-order rate constants range from 3×10^7 to 1.1×10^9 M^{-1} s^{-1}. The rate constants for the tripeptides and tripeptide amides fit a Marcus plot corresponding to an apparent self-exchange rate constant greater than 10^8 M^{-1} s^{-1} for Cu(III)–Cu(II). However, this is more than 3 orders of magnitude larger than the directly determined self-exchange rate constant for these complexes and indicates a different mechanism for the iridium–copper cross-exchange reactions. A chloride bridge between iridium and copper is proposed. The rate constants reach limiting values as the free energy change becomes more favorable. The limiting values are consistent with an inner-sphere mechanism with substitution of an axial water of copper(II) by $IrCl_6^{2-}$.

Introduction

Copper(III) peptides are formed by hexachloroiridate(IV), $IrCl_6^{2-}$, oxidation of the corresponding copper(II) complexes,[1-3] but the reactions are too fast to be measured by stopped-flow techniques.[4] The recent development of a pulsed-flow instrument[5] permits the determination of rate constants for these reactions. The pulsed-flow method incorporates integrating observation of continuous flow[6,7] for short pulses using only 3–4 mL of each reagent per determination. Half-lives down to 40 μs for reactions under second-order conditions can be measured, allowing rate constants in excess of 10^9 M^{-1} s^{-1} to be determined. The present work complements the earlier study[4] of the reactions between copper(III) peptides and $IrCl_6^{3-}$ and extends the range of peptides by use of glycylglycyl-β-alanine (GGβA), the tripeptide of aminoisobutyric acid

(1) Margerum, D. W.; Chellappa, K. L.; Bossu, F. P.; Burce, G. L. *J. Am. Chem. Soc.* **1975**, *97*, 6894.
(2) Bossu, F. P.; Chellappa, K. L.; Margerum, D. W. *J. Am. Chem. Soc.* **1977**, *99*, 2195.
(3) Margerum, D. W.; Wong, L. F.; Bossu, F. P.; Chellappa, K. L.; Czarnecki, J. J.; Kirksey, S. T., Jr.; Neubecker, T. A. *Adv. Chem. Ser.* **1977**, *No. 162*, 281.
(4) Owens, G. D.; Chellappa, K. L.; Margerum, D. W. *Inorg. Chem.* **1979**, *18*, 960.
(5) Owens, G. D.; Taylor, R. W.; Ridley, T. Y.; Margerum, D. W. *Anal. Chem.* **1980**, *52*, 130.
(6) Gerischer, H.; Heim, W. *Z. Phys. Chem. (Frankfurt/Main)* **1964**, *46*, 345.
(7) Gerischer, H.; Holzwarth, J.; Seifert, D.; Strohmaier, L. *Ber. Bunsenges. Phys. Chem.* **1969**, *73*, 952.

0020-1669/81/1320-1446$01.25/0